*Korean J. Chem. Eng.*, 36(1), 1-11 (2019)
DOI: 10.1007/s11814-018-0174-x
pISSN: 0256-1115
eISSN: 1975-7220

**INVITED REVIEW PAPER**

# Recently developed methods to enhance stability of heterogeneous catalysts for conversion of biomass-derived feedstocks

**Soosan Kim*, Yiu Fai Tsang**, Eilhann E. Kwon***, Kun-Yi Andrew Lin****,†, and Jechan Lee*,†**

*Department of Environmental and Safety Engineering, Ajou University, Suwon 16499, Korea
**Department of Science and Environmental Studies, The Education University of Hong Kong, Tai Po, New Territories, Hong Kong
***Department of Environment and Energy, Sejong University, Seoul 05006, Korea
****Department of Environmental Engineering & Innovation and Development Center of Sustainable Agriculture, National Chung Hsing University, 250 Kuo-Kuang Road, Taichung, Taiwan
(*Received 2 September 2018 • accepted 16 October 2018*)

**Abstract**−Many processes for the conversion of biomass and its derivatives into value-added products (e.g., fuels and chemicals) use heterogeneous catalysts. However, the catalysts often suffer from deactivation under harsh reaction conditions, such as liquid phase at high temperatures and pressures. The catalyst deactivation is a big obstacle to developing industrially relevant biomass conversion processes, including leaching, sintering, and poisoning of metals and collapse of catalyst support. Different approaches have been applied to limit the reversible and irreversible deactivation, highly associated with the kind of catalyst, reactants, reaction conditions, etc. This review presents recent advances in strategies to stabilize heterogeneous catalysts against deactivation for biomass conversion reactions.

Keywords: Heterogeneous Catalyst, Catalyst Stability, Catalyst Deactivation, Biomass Conversion, Catalyst Design, Biorefinery

## INTRODUCTION

Fossil fuel consumption has increased rapidly to meet the high social demand since the Industrial Revolution [1]. Our obsessive dependence on fossil fuels has triggered conflicts over energy resources due to the uneven geographical distribution of fossil fuels (including non-conventional fossil fuels), leading to fluctuations in energy prices and adverse impacts on the global economy [2,3]. The massive emissions of $CO_2$ from the consumption of fossil fuels, which have been identified as the main driver of climate change, are disrupting the natural carbon cycle [4-6]. Consequently, humanity faces urgent and extensive challenges linked to climate change [7]. To curb $CO_2$ emissions, much research has been conducted to explore the potential of various types of low-carbon energy and to develop ways to promote the energy transition toward low-carbon energy [8,9].

As a result of these efforts, the use of renewable resources has been highly encouraged [10-12]. Among various renewable resources, biomass is regarded as the only renewable carbon source that is a potential substitute for fossil carbon sources [13-15]. The commercialization of biomass-based fuels and chemicals has been implemented. For example, fermentation has been optimized via long-standing practices used to produce biofuels such as bioethanol and bio-lipids [16]. However, the commercialized biomass conversion platforms are limited to fermentation processes of edible crops (e.g., cornstarch and sugarcane), resulting in the ethical dilemma of using these crops for food or fuels/chemicals [17]. To overcome this dilemma, the use of lignocellulosic biomass (i.e., non-edible biomass) as raw materials has been widely studied [18-20].

Unfortunately, the industrialization of transforming lignocellulosic biomass has not been fully implemented due to technical limitations such as insecure feedstock supplies and high operation and maintenance costs [21]. Among those limitations, stability of heterogeneous catalysts is one of the most critical issues because the catalysts have been extensively used for many biomass conversion processes to make fuels and chemicals [22,23]. Among different categories of the catalysts, metal particles supported on oxide are particularly important because they are used in hydrotreating biomass-derived feedstocks (e.g., hydrodeoxygenation and hydrogenation), which is crucial to remove oxygen from the feedstocks [24].

Although catalytic activity and selectivity for the reactions are important to develop the processes that are to compete with petrochemical processes, catalyst stability must be guaranteed for long-term operations under real industrial conditions [25]. However, research on the long-term operations of the catalysts has been lacking for most of the biomass conversion processes, compared to that on the improvements in activity and selectivity. Therefore, it is necessary to review recent advances in technologies for stabilizing heterogeneous catalysts for conversion of biomass-derived feedstocks in order to make the biomass conversion processes more economically and industrially viable. To this end, major causes of catalyst deactivation are outlined first. Then, the efforts to stabilize different catalytic systems for transforming biomass-derived feedstocks are discussed. Finally, the challenges of advancing the biomass-based

†To whom correspondence should be addressed.
E-mail: jlee83@ajou.ac.kr, linky@nchu.edu.tw

industries are highlighted.

## CATALYST DEACTIVATION

In a heterogeneously catalyzed reaction, the catalyst can lose its activity and/or selectivity as the reaction proceeds. In other words, catalyst deactivation is the loss of activity and/or selectivity of the catalyst over reaction time. It can be classified mainly into three categories: mechanical, chemical, and thermal deactivation [26]. Physical deactivation includes fouling and attrition/crushing/erosion. Poisoning and leaching are considered chemical deactivation. Thermally induced deactivation (phase transformation and sintering) results in loss of catalytic surface area. In this section, each type of deactivation, that often takes place in biomass conversion reactions, will be briefly reviewed before starting the discussion about the technologies to reduce/prevent the catalyst deactivation in section 3.

### 1. Mechanical Deactivation

In a reaction, fouling occurs when species in the fluid stream physically deposit onto the catalyst surface. This leads to a loss of catalytic activity by the species blocking active sites (e.g., metal sites) and/or pores (e.g., pores in the catalyst support). For supported metal catalysts, fouling by coke formation or carbon deposition causes blocking of surface metal sites, plugging of pores in the support, and encapsulation of crystallite [27-29]. In an advanced stage of fouling on supported metal catalysts, the catalyst support can be stressed and fractured by strong carbon filaments building up in the pores, leading to plugging of void spaces in the reactor [30]. Physical deposition of coke or carbon in porous catalytic materials is an example of fouling. Note that chemisorption of condensed hydrocarbons (e.g., tar) can be involved in the formation of coke and carbon on the surface, poisoning catalytic sites. In fouling, carbon results from disproportion of carbon monoxide, whereas coke results from condensation or decomposition of hydrocarbons [29, 31]. Chemical structures of carbons and cokes deposited on catalyst depend on the type of reaction, reaction condition, and the kind of catalyst [32,33].

Attrition, crushing, and erosion of catalysts are other forms of mechanical deactivation. Attrition is the reduction of size of catalyst pellets (or granules) to fine particles. Decrease in the particle size and/or smoothing of the particles observed by microscopes are evidence of attrition. When the attrited catalyst accumulates in the catalyst bed of a reactor, a large increase in pressure drop occurs [26]. Crushing of monolithic, granular, or pelletized catalyst occurs because of a load. Mechanical stresses by a high fluid velocity can cause erosion of catalyst particles and/or monolith coating. The erosion may be attributed to collisions between the particles and/or between the particles and reactor walls and cavitation at the high fluid velocity [26,34].

### 2. Chemical Deactivation

Strong chemisorption of species in reactants, products, and/or impurities onto catalytic sites can poison the sites by blockage in the catalytic active sites, called poisoning [35,36]. Note that poisoning is an operational definition. A species acting as a poison is highly associated with its chemisorption strength that is relative to the other species, which competes for active sites. As an example, oxygen is a poison for ammonia synthesis [37], but a reactant for methane oxidation [38]. Also, oxygen can act as a poison for ethylene hydrogenation over a nickel (Ni) catalyst [39], while it is a reactant for ethylene oxidation over a silver catalyst [40]. The chemisorbed species (i.e., poison) can also lead to changing geometric and/or electronic structure of the catalyst surface [41,42]. Sulfur poisoning is one of the most important examples. In many industrial-scale catalytic reactors, it is a serious problem. In general, metal catalysts (e.g., Ni) are poisoned by $H_2S$ [43,44]. As mentioned, chemisorption of hydrocarbons on the catalytic sites is also considered poisoning (i.e., coking).

Poisoning by certain poisons (e.g., coke) can be removed via heating the catalyst in the presence of reductive or oxidative media forming volatile species from the carbon. Nevertheless, some supported catalysts, such as carbon-supported catalysts, are not compatible with regeneration treatment because such support material is not thermally stable, thereby degrading during the regeneration. More importantly, catalytic processes that require periodic regeneration of the catalyst are not preferred from practical and economic points of view. Thus, several methods have been proposed to alleviate catalyst deactivation due to poisoning, as it will be discussed in section 3.

Leaching, one of the most critical issues for the stability of supported metal catalysts in liquid-phase reactions, is loss of catalytic sites (metal sites) by undesirable extraction of metal atoms from the metal particles into the fluid stream. It leads not only to significant decreasing catalytic activity, but also to contaminating product stream. Leaching occurs via the formation of free metal ions [45,46].

### 3. Thermal Deactivation

Thermally induced catalyst deactivation includes transformation of catalytic phases into non-catalytic phases and sintering, such as loss of catalytic surface area by growth in crystallite and by re-growth in the catalytic surface area. Both deactivations typically occur on supported metal catalysts. A representative example of phase transformation is the formation of Ni aluminate via the reaction of Ni and alumina ($Al_2O_3$) on $Al_2O_3$-supported Ni catalysts [47-49].

Sintering happens generally at high temperatures above 500 °C [50,51], expedited in the existence of water vapor [52,53]. Sintering can take place via two mechanisms. First, is the migration of the particles over the surface of catalyst support, causing collision and coalescence forming large particles [54,55]. Second, Ostwald ripening, adatom migration minimizing free energy due to evolution of particle size and geometry [56,57]. Sintering rapidly occurring in the early stage of reaction is likely due to Ostwald ripening. With disappearance of small particles, however, the first mechanism becomes preponderant [58]. Table 1 gives a summary of catalyst deactivation discussed in this section.

## IMPROVEMENT IN CATALYST STABILITY FOR BIOMASS CONVERSION REACTIONS BY DIFFERENT METHODS

### 1. Improvement in Catalyst Stability by Atomic Layer Deposition

Atomic layer deposition (ALD), a subset of chemical vapor deposition (CVD), is a technique to grow layers on a substrate. The deposition process is performed by discrete pulsing of vapor-phase

**Table 1. Summary of catalyst deactivation in biomass conversion reactions**

| Classification | Deactivation | Description |
|---|---|---|
| Mechanical | Fouling | Coke formation or carbon deposition causing blocking of surface metal sites |
| | Attrition | Abrasion causing loss of catalytic material |
| | Crushing | Crushing of catalyst particles causing loss of internal surface area |
| | Erosion | Collisions between the particles and/or between the particles and reactor walls and cavitation |
| Chemical | Poisoning | Strong chemisorption of carbonaceous species in reactants, products, and/or impurities onto catalytic sites |
| | Leaching | Loss of catalytic sites (metal sites) by undesirable extraction of metal atoms from the metal particles into the fluid stream |
| Thermal | Phase transformation | Transformation of catalytic phases into non-catalytic phases |
| | Sintering | Loss of catalytic surface area and support area induced by heat |

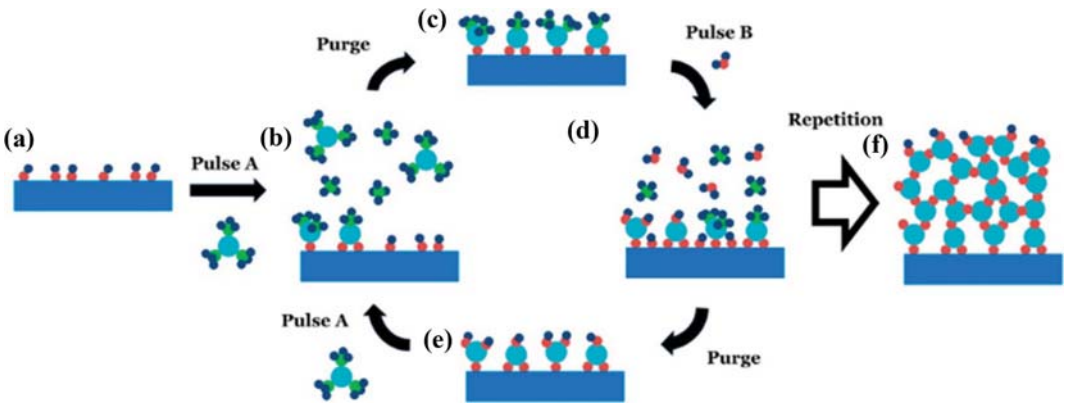


**Fig. 1. Schematic diagram of ALD on a substrate using two precursors (pulses A and B). Reprinted with permission from O'Neill et al. [59]. Copyright (2015) American Chemical Society.**

precursors acting as chemical sources of elements that constitute the layers. Fig. 1 shows a schematic representation of ALD of layers on a substrate using two chemical precursors [59]. Fig. 1(a) shows the substrate with sites with which the precursors react. Fig. 1(b) is pulsing of the first chemical precursor reacting with the reactive sites on the substrate. Typically, the precursor is a metal precursor with a high vapor pressure (e.g., titanium isopropoxide [60], titanium tetrachloride [61], hafnium tetrachloride [62], and trimethylaluminum (TMA) [63,64]) because ALD occurs under gaseous phase. The surface reaction results in the formation of surface byproducts, and remaining gaseous byproducts and unreacted precursor need to be purged (Fig. 1(c)). After the purging, the second chemical precursor then reacts with the surface (Fig. 1(d)). After the second pulsing, unreacted reactants and remaining products are again purged (Fig. 1(e)). This cycle is repeated until a desired thickness of the film is obtained, as shown in Fig. 1(f).

Many research groups have attempted stabilizing supported metal catalysts by using the ALD technique to synthesize heterogeneous catalysts that have an enhanced stability against deactivation. One of the recent strategies to apply ALD to synthesize supported metal catalysts is to deposit a film onto the catalyst surface. The protective film prevents chemical and thermal deactivation such as leaching and sintering of metal nanoparticles. Stair and co-workers overcoated $Al_2O_3$ (thickness: ~8 nm) on the surface of an $\gamma$-$Al_2O_3$-supported palladium (Pd) catalyst formed through 45 cycles of ALD using water and TMA as the precursors [65]. Once coated with the ALD film, the Pd sites are not accessible because the ALD overcoat completely covers the Pd particles. To make reactants accessible to the Pd particles, an activation is required to make microporosity (pore size: ~2 nm) inside the ALD $Al_2O_3$ overcoat by heating at 700 °C. For gaseous-phase oxidative ethane dehydrogenation conducted at 675 °C, the ALD $Al_2O_3$ overcoat greatly reduces coke formation and sintering, thereby allowing a more than ten-times higher desired product (ethylene) yield than the uncoated Pd catalyst, which suffered from coking and sintering under comparable reaction conditions.

The same approach was applied to stabilizing a copper (Cu) nanoparticles supported on $\gamma$-$Al_2O_3$ in liquid-phase furfural hydrogenation reaction by O'Neill et al. [66]. The authors made an $Al_2O_3$ overcoat over the surface of the Cu/$\gamma$-$Al_2O_3$ catalyst with 45 cycles of ALD reaction between TMA and water. The ALD $Al_2O_3$ overcoat encapsulated the Cu nanoparticles, and the ALD overcoat became porous after heat treatment at 700 °C. Catalytic performance of the uncoated Cu and ALD-coated Cu catalysts was compared for liquid-phase hydrogenation of furfural at 130 °C and 2.2 MPa $H_2$. Furfural is a commonly used model compound for biomass conversion because it is industrially derived from the hemicellulose fraction of lignocellulosic biomass [67-69]. As shown in Fig. 2,

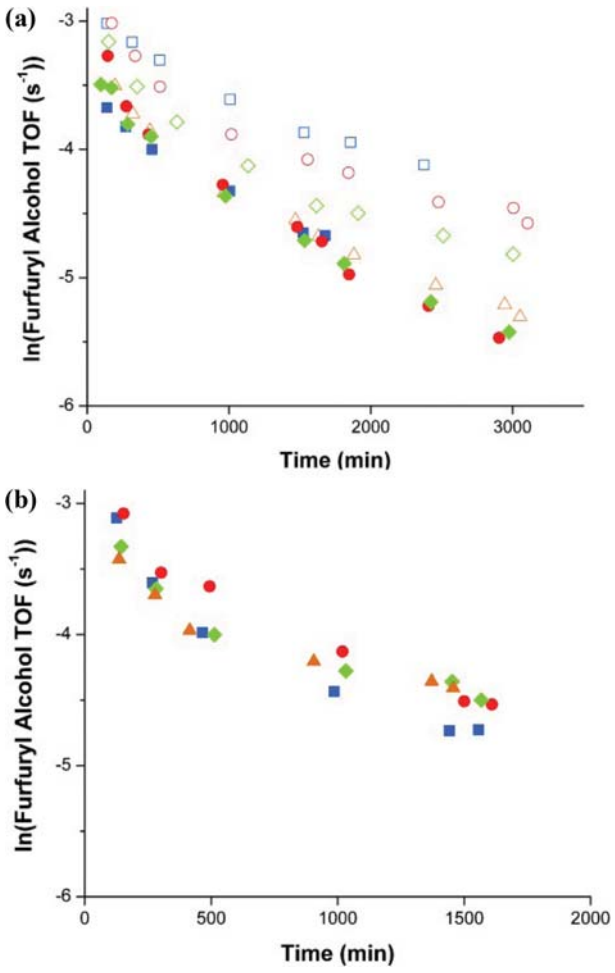


**Fig. 2. (a) Turnover frequency (TOF) in hydrogenation of furfural into furfuryl alcohol in 1-butanol over the uncoated Cu/$\gamma$-$Al_2O_3$ (hollow symbols) and ALD $Al_2O_3$ overcoated Cu/$\gamma$-$Al_2O_3$ (solid symbols) catalysts. (b) TOF in hydrogenation of furfural into furfuryl alcohol in water over the ALD $Al_2O_3$ overcoated Cu/$\gamma$-$Al_2O_3$ catalyst (□: fresh; ○: 1st regeneration; ◇: 2nd regeneration; △: 3rd regeneration). Reproduced with permission from O'Neill et al. [66], Copyright 2013 John Wiley and Sons.**

a loss of catalytic activity was observed for both catalysts as the reaction proceeded. However, deactivation of the uncoated catalyst was not reversible after regeneration (i.e., *in situ* calcination and reduction), while that of the ALD coated catalyst was reversible. The reversible deactivation occurring on the ALD Cu catalyst was due to coke formation; however, in addition to coking the uncoated catalyst experienced irreversible deactivation such as leaching and sintering during the reaction, confirmed with catalyst characterization via inductively coupled plasma atomic emission spectroscopy (ICP-OES) and scanning transmission electron microscopy (STEM). The ALD $Al_2O_3$ overcoat prevented leaching and sintering of the Cu particles in harsh liquid-phase reaction conditions (e.g., hot water and high pressure). Given that leaching and sintering of metal particles originate from metal atoms at corners, edges, and defects (under-coordinated metal atoms) [70,71], it was hypothesized that the ALD $Al_2O_3$ overcoat selectively interacts with under-coordinated surface Cu atoms, resulting in stabilizing the catalyst. The ALD $Al_2O_3$ film also successfully stabilized Cu chromite catalysts for gas-phase furfural hydrogenation [72,73].

The ALD $Al_2O_3$ overcoat prevented leaching and sintering, but it could not prevent the deposition of coke, although it is reversible deactivation as discussed earlier. O'Neill et al. tried to limit coking by chemically modifying the $Al_2O_3$ overcoat [74]. The acidity of the overcoat was decreased by the addition of basic $MgO_x$. Considering the acidity may expedite coke formation, the $MgO_x$-modified ALD $Al_2O_3$ Cu/$\gamma$-$Al_2O_3$ catalyst underwent a lower deposition of coke than the ALD $Al_2O_3$ Cu/$\gamma$-$Al_2O_3$ catalyst without adding $MgO_x$, while the stabilization of the Cu particles was still provided (stable against leaching and sintering). However, a pure $MgO_x$-overcoated Cu/$\gamma$-$Al_2O_3$ catalyst was not stable against leaching and sintering.

Other than $Al_2O_3$ overcoating by ALD, a titania ($TiO_2$) overcoat (30 cycles of ALD using titanium tetrachloride and water; thickness of ~1.2 nm) was formed on a cobalt (Co) catalyst supported on $TiO_2$ to stabilize the Co particles in aqueous-phase hydrogenation of furfural, furfuryl alcohol, and xylose [75]. The ALD $Al_2O_3$ coating did not work for the Co catalyst because inactive Co aluminate (not reducible up to 800 °C confirmed with characterization by hydrogen-temperature programmed reduction ($H_2$-TPR)) was formed during the heat treatment required to open pores inside the overcoat. Therefore, ALD $TiO_2$ overcoated Co/$TiO_2$ catalyst was prepared and compared with an uncoated Co/$TiO_2$ catalyst. The $H_2$-TPR characterization showed the $TiO_2$ overcoated catalyst was reducible at 600 °C. While the traditional catalyst without the ALD overcoat lost about 10% of its Co by leaching for 35-h reaction, the Co loading of the ALD catalyst did not change after a couple of regenerations. In addition, transmission electron microscopy (TEM) characterization revealed that no sintering occurred after two regenerations of the ALD $TiO_2$-coated Co/$TiO_2$ catalyst. Another study also showed a $TiO_2$ overcoat made via ALD with titanium isopropoxide and water could stabilize a commercial Cu chromite catalyst for furfural hydrogenation reaction by preventing the formation of coke and the migration of chromite leading to blockage of Cu sites [76,77].

The ALD technique was also used to synthesize hydrothermally stable oxide catalysts. Pagán-Torres et al. conducted ALD of niobia ($Nb_2O_5$) within the pores of a silica (mesoporous SBA-15) by changing ALD cycles from 10 to 30 [78]. Niobium(V) ethoxide and water were used as the ALD $Nb_2O_5$ precursors. An increase in $Nb_2O_5$ loading decreased surface area, pore size, and pore volume, resulting from the conformal coating of $Nb_2O_5$ over the surface. The catalysts made with 10, 19, and 30 ALD $Nb_2O_5$ cycles were hydrothermally stable, demonstrated by marginal changes in structural properties and porosity after hydrothermal treatments in water at 200 °C for 12 h. The acid catalyst with 19 cycles of ALD $Nb_2O_5$ was also tested for dehydration of isopropyl alcohol and 2-butanol in gas and liquid phases. The catalytic activity (based on mass of catalyst) of the ALD catalyst was superior to a commercial $Nb_2O_5$ catalyst (HY-340). In addition to the acid-catalyzed dehydration reactions, the ALD $Nb_2O_5$ catalyst was used as a catalyst support. Pd nanoparticles were dispersed on the ALD $Nb_2O_5$ coted on SBA-15 (19 cycles) and the Pd/ALD $Nb_2O_5$/SBA-15 cata-

lyst was used to convert γ-valerolactone (GVL) into pentanoic acid. The conversion of GVL into pentanoic acid has been considered a promising reaction in biorefinery [79-81]. The Pd/ALD $Nb_2O_5$/SBA-15 catalyst and the commercial HY-340 supported Pd catalyst (Pd/HY-340) were evaluated in a continuous flow reactor. The catalytic activity versus time-on-stream data demonstrated that the Pd/ALD $Nb_2O_5$/SBA-15 catalyst is more stable than the Pd/HY-340 catalyst for the GVL conversion reaction.

**2. Improvement in Catalyst Stability by Strong Metal-support Interaction**

Strong metal-support interaction (SMSI) is known to be responsible for catalytic activity, selectivity, and stability. Hence, research on SMSI has recently gained interest for developing a new class of heterogeneous catalytic systems [82]. The SMSI effect is attributed to partially reduced metal oxide species migrating onto the metal surface [83-85]. For example, the SMSI occurring on Ni/$TiO_2$ catalyst was observed by *in situ* STEM [86]. More recently, depth-sensitive X-ray photoelectron spectroscopy (XPS) characterization was used to probe the coverage of Cu particles by a zinc oxide ($ZnO_x$) layer [87]. The SMSI has been exploited to design different catalytic systems such as oxidation of carbon monoxide (CO) over Pd catalysts [88], synthesis of methanol over Cu catalysts [87], production of hydrogen over platinum (Pt) catalysts [89], hydrogenation of carbon dioxide ($CO_2$) over Co catalysts [90], and hydrogenation of furfural over Pt catalysts [91]. Nevertheless, most studies of SMSI have emphasized the enhancement of activity and/or selectivity.

Exploitation of SMSI was suggested by Huber and co-workers, as a simple inexpensive method to make stable base metal catalysts (e.g., Co particles supported on $TiO_2$ (Co/$TiO_2$)) for aqueous-phase hydrogenation of biomass-derived oxygenates (e.g., furfuryl alcohol) at 140 °C [92]. The authors first prepared Co particles supported on $TiO_2$ (Co/$TiO_2$) by incipient wetness impregnation, and then treated the Co/$TiO_2$ catalyst via a series of calcination and reduction at high temperatures (450 or 600 °C). The reduction at 600 °C induced SMSI in the system, a $TiO_y$ layer covering the Co particles. The SMSI was demonstrated by *in situ* Raman spectroscopy and STEM characterization, as shown in Fig. 3. The SMSI $TiO_y$-coverd Co/$TiO_2$ catalyst did not undergo Co leaching, while the Co/$TiO_2$ catalyst reduced at 450 °C lost 44.6% of Co during the reaction for 35 h. However, the study used a diluted feedstock (2 wt% aqueous solutions). Eagan et al. observed that a Co/$TiO_2$ catalyst treated by a same way (i.e., heat treatments at 600 °C) suffered from irreversible deactivation such as leaching and sintering at harsher reaction conditions (268 °C) with a more concentrated feedstock (20 wt% aqueous solution) [93]. The feedstock (sorbitol;

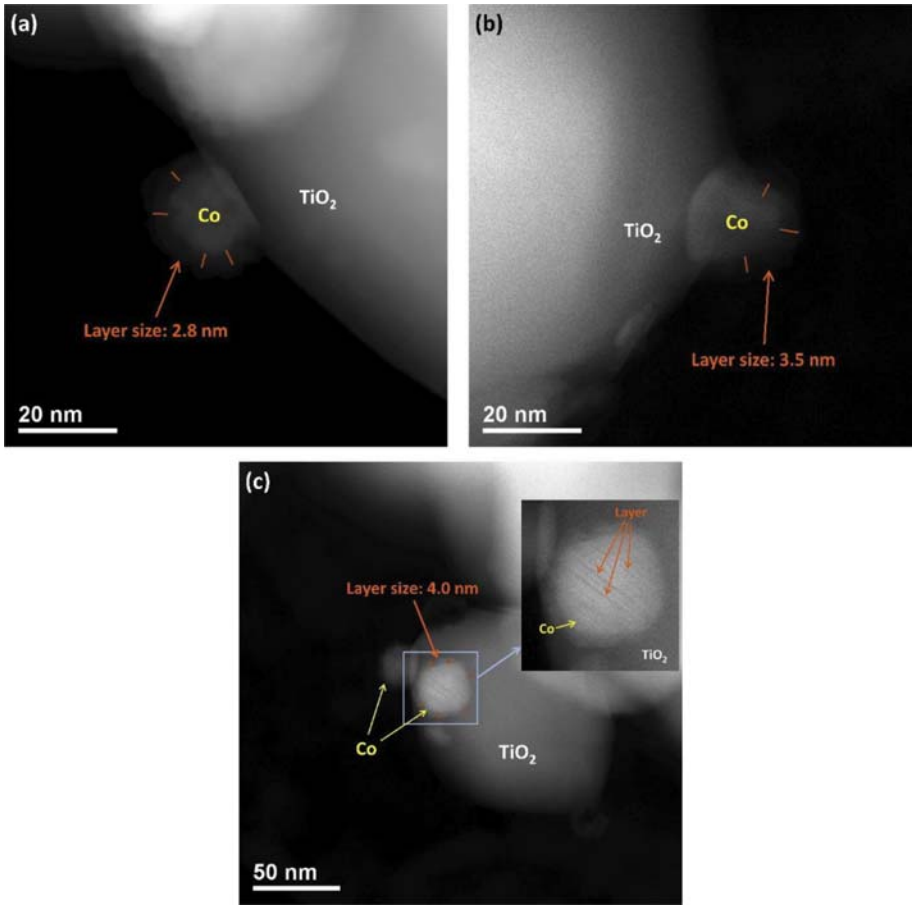


**Fig. 3. STEM images of (a) Co/$TiO_2$ after reduction at 600 °C, (b) Co/$TiO_2$ after calcination at 400 °C and then reduction at 600 °C, and (c) Co/$TiO_2$ after calcination at 600 °C and then reduction at 600 °C. Reprinted from Lee et al. [92], Copyright (2015), with permission from Elsevier.**

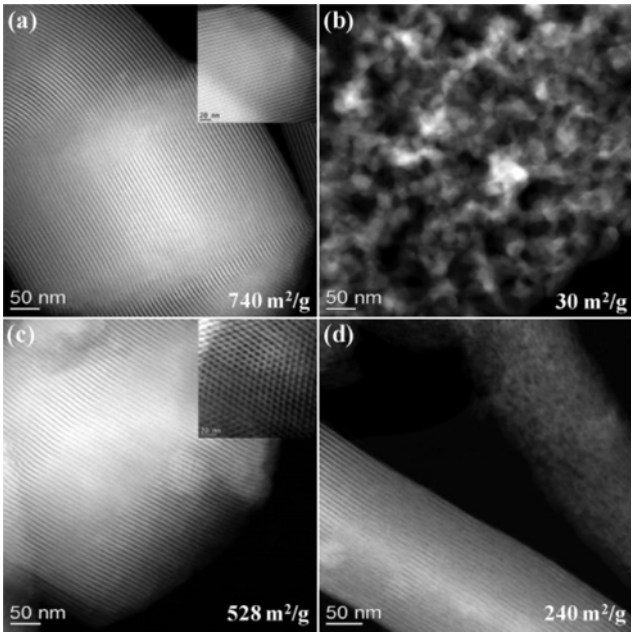


**Fig. 4. STEM images of (a) SBA-15, (b) SBA-15 after hydrothermal treatment, (c) carbon-coated SBA-15, and (d) carbon-coated SBA-15 after hydrothermal treatment. Reproduced with permission from Pham et al. [94], Copyright 2012 John Wiley and Sons.**

O/C=1) was also more highly oxygenated than furfuryl alcohol (O/C=0.4). This indicates that the characteristic of oxygenated feedstocks and reaction conditions likely affects catalyst stability for biomass conversion reactions.

### 3. Improvement in Catalyst Stability by Other Film Deposition Techniques

Hydrothermal stability of mesoporous oxides such as $SiO_2$ and $Al_2O_3$ at temperatures higher than 100 °C (e.g., 200 °C) was enhanced by depositing a thin carbon film (~10 wt%) using sucrose as the carbon source [94]. An aqueous sucrose solution was added to an oxide (fumed $Al_2O_3$, $SiO_2$ gel, or SBA-15), followed by drying to remove water. The dried sucrose-oxide mixture was pyrolyzed at 400 °C for 2 h under nitrogen ($N_2$) atmosphere. Fig. 4 presents STEM images of the carbon-deposited SBA-15 before and after hydrothermal treatment conducted at 200 °C for 12 h. As shown in Fig. 4, the SBA-15 without carbon coating lost not only 96% of surface area due to a collapse of mesopores, but also its structural integrity. However, the carbon-coated one lost only 55% of surface area with an ordered mesoporous structure that was partially retained after hot water treatment. Similar phenomena were observed in the fumed $Al_2O_3$ and $SiO_2$ gel. The results clearly indicate that the carbon coating on mesoporous oxides via pyrolysis of simple sugar stabilizes the oxides.

Xiong et al. developed a deposition-precipitation-carbonization method to synthesize hydrothermally stable $Nb_2O_5$/carbon composite [95]. To make the catalytic material, ammonium niobium oxalate was reacted with glucose in the presence of urea (to control pH by its decomposition) in a batch reactor at 200 °C for 12 h, followed by drying. After drying, the mixture was pyrolyzed in $N_2$ at 400 °C for 6 h, yielding highly dispersed spherical particles of

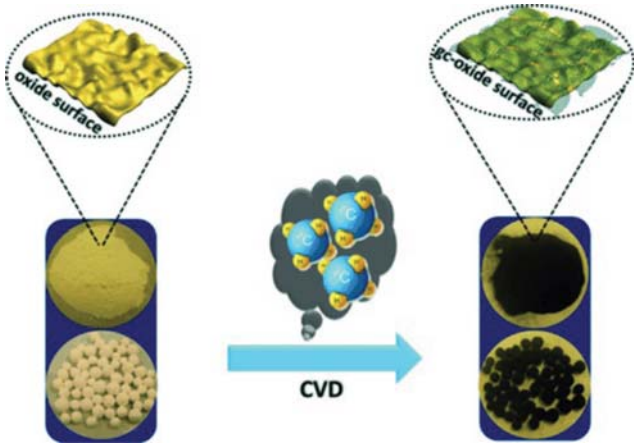


**Fig. 5. Scheme for preparing graphitic carbon/$Al_2O_3$ composite by using CVD. Reproduced with permission from Xiong et al. [97], Copyright 2015 John Wiley and Sons.**

the composite. The $Nb_2O_5$/carbon composite was more stable than a pure $Nb_2O_5$ (HY-340) in dehydration of butanol at 240 °C. The enhanced stability may be because the embedment of $Nb_2O_5$ in carbon inhibits oxide crystallite size growth during the reaction. To obtain enhanced hydrothermal stability, a strong interaction between $Nb_2O_5$ and carbon is required [96]. When the $Nb_2O_5$/carbon composite was used as the support of a Pd catalyst for transforming GVL into pentanoic acid at 300 °C, it also showed enhanced stability for ~100 h time-on-stream compared to a Pd catalyst supported on HY-340.

The same research group also deposited graphitic carbon on the surface of $\gamma$-$Al_2O_3$ by using CVD at 900 °C [97]. In the CVD process, methane was used as a reactant (Fig. 5). The loading of the carbon could be controlled by the reaction time of CVD using methane, monitored by X-ray diffraction (XRD). The uniform deposition of the graphitic carbon on the $Al_2O_3$ surface was proven by TEM, energy-filtered TEM (EFTEM), and Raman spectroscopy characterizations. Also, the graphitic carbon/$Al_2O_3$ composite showed a high degree of graphitization on the entire surface, which was not observed in either pure $Al_2O_3$ or $Al_2O_3$ covered by pyrolyzed carbon. The composite and its parent $Al_2O_3$ were treated in water at 220 °C for 12 h. The pure $Al_2O_3$ was reacted with water, forming boehmite after the treatment. However, the graphitic carbon/$Al_2O_3$ composite did not undergo a phase transformation to boehmite. In addition, surface area and porosity of the composite material were not significantly changed after the treatment, but those of the $\gamma$-$Al_2O_3$ significantly decreased (e.g., 80% loss of surface area and 90% decrease in pore volume). Pt particles supported on the graphitic carbon/$Al_2O_3$ composite were stable against leaching and sintering for aqueous-phase reforming (APR) of ethylene glycol. The graphitic carbon/$Al_2O_3$ composite-supported Ru catalyst also exhibited superior stability under acidic conditions (aqueous-phase hydrogenation of lactic acid), showing no phase transformation of the support and no sintering of Ru particles after the reaction.

A new technique to deposit thin $TiO_2$ film on catalyst surface with excellent conformality was introduced by Héroguel et al. [98], a potential alternative to ALD. In the non-hydrolytic sol-gel chem-

istry-based one-step method, mixtures of precursors (titanium isopropoxide and titanium tetrachloride) are continuously injected in liquid phase (anhydrous toluene as the solvent), resulting in forming conformal $TiO_2$ layers on the substrate (e.g., SBA-15 with a high surface area (690 $m^2$ $g^{-1}$)). The growth rate of the $TiO_2$ overcoats was 0.4 nm injected monolayer$^{-1}$. The $TiO_2$-overcoated SBA-15 was more selective (55% selectivity at 99% conversion) for dehydration of styrallyl alcohol to styrene than HZSM-5 zeolite (12% selectivity at 99% conversion) that is typically used for the dehydration reaction. However, the zeolite catalyst undergoes severe deactivation because its strong acid sites cause polymerization of styrene [99-101]. The styrene polymerization leads to the formation of styrene oligomers likely blocking catalytic sites. Recycling studies showed that the HZSM-5 catalyst deactivated much faster than the $TiO_2$-overcoated SBA-15 catalyst. $TiO_2$ was also overcoated on a Pt catalyst supported on $SiO_2$ using the same methodology ($TiO_2$/Pt/$SiO_2$). The bifunctional $TiO_2$/Pt/$SiO_2$ catalyst was tested for hydrodeoxygenation of 3-propylguaiacol that can be derived from the lignin portion of lignocellulosic biomass [102-105]. The $TiO_2$ overcoating enhanced the selectivity toward propylcyclohexane (90% selectivity at 95% conversion) compared to the uncoated Pt/$SiO_2$ catalyst (5% selectivity at 20% conversion). Also found was that the thickness of the overcoating plays an important role in the reactivity of the catalysts.

**4. Improvement in Catalyst Stability by Surface Functionalization**

Methods to stabilize zeolites by surface functionalization will be discussed next. As an example, Zapata et al. generated hydrophobicity on HY zeolite by silylation using octadecyltrichlorosilane (OTS) [106]. The created hydrophobicity on the zeolite allowed a limited contact between the surface and water, thereby preventing demolition of its structure in water/oil biphasic systems for important biofuel upgrading reactions (e.g., alkylation of *m*-cresol with 2-propanol, dehydration of 2-propanol to propylene, and dehydration of 3-pentanol to pentene). In Fig. 6, the catalytic performance of the untreated and OTS-functionalized zeolites for the alkylation reaction was compared, clearly indicating that the OTS-functionalized zeolite better catalyzes the reaction than the untreated zeolite. After the alkylation reaction for 3 h, the surface area and micropore volume of the untreated samples decreased from 690 to 215 $m^2$ $g^{-1}$ and from 0.27 to 0.01 $cm^3$ $g^{-1}$, respectively. By contrast, those of the OTS-functionalized zeolite were practically unchanged.

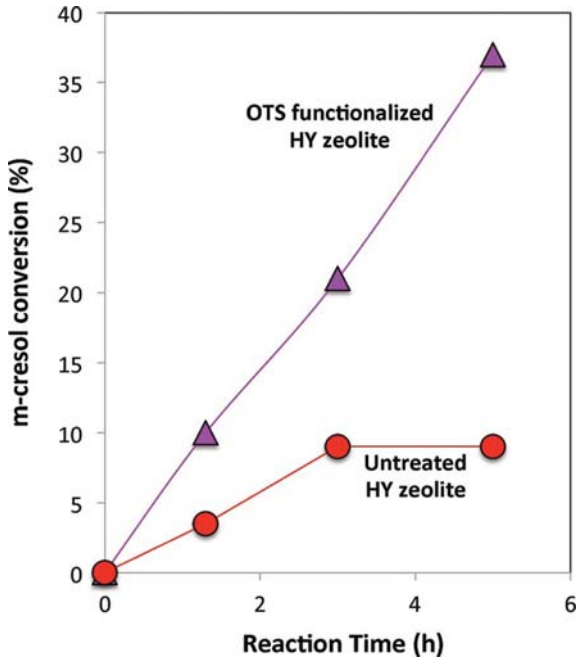


**Fig. 6. Comparison of catalytic performance of the untreated and OTS-functionalized zeolites for alkylation of *m*-cresol with 2-propanol. Reaction conditions: 200 °C, 48.3 bar He. Reprinted with permission from Zapata et al. [106]. Copyright (2012) American Chemical Society.**

A systematic study was published by the same research group using three different silylating agents, such as ethyltrichlorosilane ($C_2$), hexyltrichlorosilane ($C_6$), and OTS ($C_{18}$) [107]. Among them, ethyltrichlorosilane with a high concentration (e.g., 1.5 mmol silane per g zeolite) was most effective for the hydrophobization because its short alkyl length allows itself to reach pores and defects in the zeolite. However, the stability of the zeolite was mostly enhanced when treated with longer alkyl-chain silylating agent (e.g., octadecyltrichlorosilane) with an enhanced interaction between the organic phase and the hydrophobized zeolite that may further protect the zeolite against the water attack.

**5. Improvement in Catalyst Stability by Modification of Reaction Parameters**

In addition to improving catalyst stability by the design of catalytic materials as discussed in previous subsections, there have been efforts to prolong the lifetime of the catalysts by modifying reaction conditions.

Bitter and co-workers made carbon nanofibers-supported Ni (Ni/CNF) catalyst by a typical impregnation method and used the Ni/CNF catalyst for APR of ethylene glycol to produce $H_2$ [108]. The catalyst suffered from extreme deactivation such as the growth of Ni particle size at 230 °C under inert gaseous environment (argon (Ar)) with an initial ethylene glycol concentration of 1 wt%. The first way to stabilize the Ni/CNF catalyst was to change the gaseous atmosphere from inert gas (Ar) to more reductive gas ($H_2$). In the reductive gas environment, the growth of Ni particles was suppressed. For example, in Ar the average particle size of Ni (measured based on $H_2$ chemisorption uptake) increased from 5.9 to 61 nm, while in $H_2$ the particle size increased only to 32 nm. The loss of Ni by leaching was also decreased in the reaction conducted in $H_2$ (0.15% mass loss) compared to in Ar (0.26% mass loss). However, this kind of strategy--reaction in a more reductive gas environment--does not always work. For instance, for a graphite-supported Pt catalyst system at high pH, Pt particles agglomerated in a $H_2$-rich condition [109]. The second way to enhance stability of the Ni catalyst is to add KOH to increase pH. Note that leaching of metal nanoparticles tends to be severe at low pH values [110]. In case of Ni, the $Ni^{2+}$ species can form in acids or water at pH lower than 7 [111,112]. With the addition of KOH, a high selectivity toward $H_2$ (99%) was obtained for 50-h continuous reaction.

The control of reaction media can help prevent deactivation. Gayubo et al. reported that co-feeding 70 wt% of methanol with crude bio-oil attenuated coking on a Ni catalyst supported on

**Table 2. Summary of the recently developed methods to improve catalyst stability for biomass conversion reactions**

| Method to prevent deactivation | Catalyst | Reaction | Deactivation | Reference |
|---|---|---|---|---|
| Film deposition techniques | | | | |
| ALD | Pd/$\gamma$-$Al_2O_3$ ($Al_2O_3$ overcoat) | Gas phase dehydrogenation of ethane | Coking and sintering | [65] |
| | Cu/$\gamma$-$Al_2O_3$ ($Al_2O_3$ overcoat) | Liquid phase hydrogenation of furfural | Leaching and sintering | [66] |
| | Cu/$\gamma$-$Al_2O_3$ ($MgO_x$-$Al_2O_3$ overcoat) | Liquid phase hydrogenation of furfural | Coking | [74] |
| | Co/$TiO_2$ ($TiO_2$ overcoat) | Aqueous phase hydrogenation of furfuryl alcohol | Leaching and sintering | [75] |
| | Pd/SBA-15 ($Nb_2O_5$ overcoat) | Conversion of GVL into pentanoic acid | Support dissolution | [78] |
| SMSI | Co/$TiO_2$ ($TiO_y$ overlayer) | Aqueous phase hydrogenation of furfuryl alcohol | Leaching and sintering | [92] |
| Pyrolysis of sugar | Pd/$SiO_2$ and Pd/$Al_2O_3$ (carbon film) | Hydrogenation of acetylene/ethylene | Support dissolution | [94] |
| CVD | Pt/$\gamma$-$Al_2O_3$ (carbon coating) | APR of ethylene glycol | Leaching, sintering, and support dissolution | [97] |
| | Ru/$\gamma$-$Al_2O_3$ (carbon coating) | Aqueous-phase hydrogenation of lactic acid | Sintering and support dissolution | [97] |
| Non-hydrolytic sol-gel chemistry-based deposition | SBA-15 ($TiO_2$ film) | Dehydration of styrallyl alcohol | Carbon poisoning | [98] |
| Surface functionalization | | | | |
| Functionalization using silylation with OTS | HY zeolite | Alkylation and dehydration | Support dissolution | [106] |
| Modifying reaction parameters | | | | |
| Using reductive gas agent ($H_2$) | Ni/CNF | APR of ethylene glycol | Leaching and sintering | [108] |
| Adding KOH | Ni/CNF | APR of ethylene glycol | Leaching and sintering | [108] |
| Co-feeding methanol | Ni/HZSM-5 | Upgrading crude bio-oil | Coking | [113] |
| Reaction in a biphasic system consisting of water and MIBK | Ga/USY zeolite | Aqueous phase isomerization of xylose | Leaching and support dissolution | [114] |

HZSM-5 that was used for upgrading the bio-oil [113]. The methanol co-feeding mostly hindered the formation of thermal coke derived from polymerization of phenolic species in the bio-oil (i.e., pyrolytic lignin) rather than catalytic coke derived from acid-catalyzed oxygenates. An USY zeolite-supported gallium (Ga) (Ga/USY) catalyst suffered from severe Ga leaching during aqueous phase isomerization of xylose at 130 °C for 24 h (Ga loading was decreased from 5.9 to 0.27 wt%) [114]. To prevent deactivation, the authors used the biphasic system consisting of 20% water and 80% methyl isobutyl ketone (MIBK). In the biphasic medium, Ga leaching was suppressed (Ga loading was decreased from 5.9 to 2.1 wt%) while the zeolite crystallinity was maintained. Table 2 summarizes the methods to improve catalyst stability, reviewed in this section.

## CONCLUSIONS AND PROSPECTS

Catalyst deactivation is the main bottleneck to biomass conversion processes competing with petrochemical processes. To help resolve this issue, this review presented recently applied approaches, including film deposition techniques (ALD, SMSI, CVD, pyrolysis of sugar, etc.), surface functionalization, and modification of reaction parameters, in order to increase lifetime of heterogeneous catalysts for the reactions to transform biomass-derived feedstocks. Even though some methods have been successful in reducing or preventing the deactivation phenomena for the reactions of model compounds as presented above, stabilization of catalysts for the processes to treat real biomass is not fully studied or even not tested. In addition, a number of reactions occur simultaneously in a biomass conversion reaction [115,116] resulting from biomass feedstocks having complex functionalities [117]. This necessarily results in biomass conversion processes to require the use of bifunctional catalysts which have different catalytic sites in one catalyst. However, different catalytic sites are deactivated in different ways, causing considerable difficulties in design strategies for enhancing

the catalyst stability in the biomass conversion reactions. Hence, investigations of the bifunctional catalyst stability with real feed solutions directly derived from lignocellulosic biomass would be most instructive. The presence of impurities contained in the real biomass feed stream might have serious effects on the catalyst in long-term operations.

Furthermore, current techniques for synthesizing heterogeneous catalysts allow precise control of nanostructured catalytic active sites. Despite the technological progress in catalyst synthesis, reaction conditions of biomass conversion technologies are harsh compared to other industrial catalytic processes. Future researches should combine the above-mentioned techniques and principles to further develop more advanced technologies to stabilize catalysts in biomass conversion. The stabilized catalytic processes would greatly help in developing sustainable routes to renewable carbon-based products.

## ACKNOWLEDGEMENTS

This work was supported by a National Research Foundation of Korea (NRF) Grant funded by the Korean Government (Ministry of Education) (No. 2018R1D1A1A09082841).

## REFERENCES

1. S. Chu and A. Majumdar, *Nature*, **488**, 294 (2012).
2. S. P. A. Brown and M. K. Yücel, *The Quarterly Review of Economics and Finance*, **42**, 193 (2002).
3. M. A. Brown, *Energy Policy*, **29**, 1197 (2001).
4. V. Ramanathan and Y. Feng, *Atmospheric Environ.*, **43**, 37 (2009).
5. T. W. R. Powell and T. M. Lenton, *Energy Environ. Sci.*, **5**, 8116 (2012).
6. N. S. A. Rasid, S. S. A. Syed-Hassan, S. A. S. A. Kadir and M. Asadullah, *Korean J. Chem. Eng.*, **30**, 1277 (2013).
7. H. P. Jones, D. G. Hole and E. S. Zavaleta, *Nat. Clim. Change*, **2**, 504 (2012).
8. H. C. McJeon, L. Clarke, P. Kyle, M. Wise, A. Hackbarth, B. P. Bryant and R. J. Lempert, *Energy Econ.*, **33**, 619 (2011).
9. V. Albino, L. Ardito, R. M. Dangelico and A. M. Petruzzelli, *Appl. Energy*, **135**, 836 (2014).
10. A. Behr and J. P. Gomes, *Eur. J. Lipid Sci. Technol.*, **112**, 31 (2010).
11. S. Cho and J. Kim, *Korean J. Chem. Eng.*, **33**, 2808 (2016).
12. M. Song, H. D. Pham, J. Seon and H. C. Woo, *Korean J. Chem. Eng.*, **32**, 567 (2015).
13. A. Baral and G. S. Guha, *Biomass Bioenergy*, **27**, 41 (2004).
14. C. H. Ko, S. H. Park, J.-K. Jeon, D. J. Suh, K.-E. Jeong and Y.-K. Park, *Korean J. Chem. Eng.*, **29**, 1657 (2012).
15. H. Lee, Y.-M. Kim, I.-G. Lee, J.-K. Jeon, S.-C. Jung, J. D. Chung, W. G. Choi and Y.-K. Park, *Korean J. Chem. Eng.*, **33**, 3299 (2016).
16. A. M. Henstra, J. Sipma, A. Rinzema and A. J. Stams, *Curr. Opin. Biotechnol.*, **18**, 200 (2007).
17. M. Martín, *Energy Res. J.*, **5**, 1 (2014).
18. R. Kumar, S. Singh and O. V. Singh, *J. Ind. Microbiol. Biotechnol.*, **35**, 377 (2008).
19. Y. Lee, H. Shafaghat, J.-k. Kim, J.-K. Jeon, S.-C. Jung, I.-G. Lee and Y.-K. Park, *Korean J. Chem. Eng.*, **34**, 2180 (2017).
20. H. Kim, H. Shafaghat, J.-k. Kim, B. S. Kang, J.-K. Jeon, S.-C. Jung, I.-G. Lee and Y.-K. Park, *Korean J. Chem. Eng.*, **35**, 922 (2018).
21. K. Srirangan, L. Akawi, M. Moo-Young and C. P. Chou, *Appl. Energy*, **100**, 172 (2012).
22. Y.-C. Lin and G. W. Huber, *Energy Environ. Sci.*, **2**, 68 (2009).
23. H. Xiong, H. N. Pham and A. K. Datye, *Green Chem.*, **16**, 4627 (2014).
24. J. Wildschut, F. H. Mahfud, R. H. Venderbosch and H. J. Heeres, *Ind. Eng. Chem. Res.*, **48**, 10324 (2009).
25. G. C. de Araújo and M. do Carmo Rangel, *Catal. Today*, **62**, 201 (2000).
26. C. H. Bartholomew, *Appl. Catal. A-Gen.*, **212**, 17 (2001).
27. D. L. Trimm, *Catal. Rev.*, **16**, 155 (1977).
28. S. M. Davis, F. Zaera and G. A. Somorjai, *J. Catal.*, **77**, 439 (1982).
29. R. S. Ruoff, D. C. Lorents, B. Chan, R. Malhotra and S. Subramoney, *Science*, **259**, 346 (1993).
30. C. H. Bartholomew, *Chem. Eng.*, **91**, 96 (1984).
31. J. Guo, H. Lou and X. Zheng, *Carbon*, **45**, 1314 (2007).
32. P. G. Menon, *J. Mol. Catal.*, **59**, 207 (1990).
33. M. D. Argyle and C. H. Bartholomew, *Catalysts*, **5**, 145 (2015).
34. S. Kuroda, J. Kawakita, M. Watanabe and H. Katanoda, *Sci. Technol. Adv. Mater.*, **9**, 033002 (2008).
35. D. L. Trimm, *Appl. Catal. A-Gen.*, **212**, 153 (2001).
36. R. Zhang, F. Li, N. Zhang and Q. Shi, *Appl. Catal. A-Gen.*, **239**, 17 (2003).
37. J. A. Almquist and C. A. Black, *J. Am. Chem. Soc.*, **48**, 2814 (1926).
38. M. Lyubovsky and L. Pfefferle, *Catal. Today*, **47**, 29 (1999).
39. H.-P. Koh and R. Hughes, *J. Catal.*, **33**, 7 (1974).
40. E. L. Force and A. T. Bell, *J. Catal.*, **40**, 356 (1975).
41. L. L. Hegedus and R. W. McCabe, Catalyst Poisoning, in: B. Delmon, G. F. Froment (Eds.) Studies in Surface Science and Catalysis, Elsevier, 471 (1980).
42. C. H. Bartholomew, Mechanisms of Nickel Catalyst Poisoning, in: B. Delmon, G. F. Froment (Eds.) Studies in Surface Science and Catalysis, Elsevier, 81 (1987).
43. F. S. Karn, J. F. Schultz, R. E. Kelly and R. B. Anderson, *Ind. Eng. Chem. Prod. Res. Dev.*, **2**, 43 (1963).
44. H. Ago, T. Komatsu, S. Ohshima, Y. Kuriki and M. Yumura, *Appl. Phys. Lett.*, **77**, 79 (2000).
45. M. Hartmann and S. Ernst, *Angew. Chem., Int. Ed.*, **39**, 888 (2000).
46. J. J. Dijkstra, J. C. L. Meeussen and R. N. J. Comans, *Environ. Sci. Technol.*, **38**, 4390 (2004).
47. K.-i. Shimizu, A. Satsuma and T. Hattori, *Catal. Surv. Jpn.*, **4**, 115 (2001).
48. T. de Freitas Silva, J. A. C. Dias, C. G. Maciel and J. M. Assaf, *Catal. Sci. Technol.*, **3**, 635 (2013).
49. S. Sepehri and M. Rezaei, *Chem. Eng. Technol.*, **38**, 1637 (2015).
50. C. U. Jung, M.-S. Park, W. N. Kang, M.-S. Kim, K. H. Kim, S. Y. Lee and S.-I. Lee, *Appl. Phys. Lett.*, **78**, 4157 (2001).
51. P. Sharma, A. Gupta, K. V. Rao, F. J. Owens, R. Sharma, R. Ahuja, J. M. O. Guillen, B. Johansson and G. A. Gehring, *Nat. Mater.*, **2**, 673 (2003).
52. R. B. Bagwell and G. L. Messing, *J. Am. Ceram. Soc.*, **82**, 825 (1999).
53. V. Goertz, F. Weis, E. Keln, H. Nirschl and M. Seipenbusch, *Aerosol Sci. Tech.*, **45**, 1287 (2011).
54. J. Lif, M. Skoglundh and L. Löwendahl, *Appl. Catal. A-Gen.*, **228**, 145 (2002).
55. J. R. Rostrup-Nielsen, K. Pedersen and J. Sehested, *Appl. Catal. A-*

*Gen.*, **330**, 134 (2007).
56. M.-K. Kang, D.-Y. Kim and N. M. Hwang, *J. Eur. Ceram. Soc.*, **22**, 603 (2002).
57. S. B. Simonsen, I. Chorkendorff, S. Dahl, M. Skoglundh, J. Sehested and S. Helveg, *J. Catal.*, **281**, 147 (2011).
58. S. R. Challa, A. T. Delariva, T. W. Hansen, S. Helveg, J. Sehested, P. L. Hansen, F. Garzon and A. K. Datye, *J. Am. Chem. Soc.*, **133**, 20672 (2011).
59. B. J. O'Neill, D. H. K. Jackson, J. Lee, C. Canlas, P. C. Stair, C. L. Marshall, J. W. Elam, T. F. Kuech, J. A. Dumesic and G. W. Huber, *ACS Catal.*, **5**, 1804 (2015).
60. M. Ritala, M. Leskela, L. Niinisto and P. Haussalo, *Chem. Mater.*, **5**, 1174 (1993).
61. M. Ritala, M. Leskelä, E. Nykänen, P. Soininen and L. Niinistö, *Thin Solid Films*, **225**, 288 (1993).
62. J. Aarik, A. Aidla, A. A. Kiisler, T. Uustare and V. Sammelselg, *Thin Solid Films*, **340**, 110 (1999).
63. A. C. Dillon, A. W. Ott, J. D. Way and S. M. George, *Surf. Sci.*, **322**, 230 (1995).
64. G. S. Higashi and C. G. Fleming, *Appl. Phys. Lett.*, **55**, 1963 (1989).
65. J. Lu, B. Fu, M. C. Kung, G. Xiao, J. W. Elam, H. H. Kung and P. C. Stair, *Science*, **335**, 1205 (2012).
66. B. J. O'Neill, D. H. K. Jackson, A. J. Crisci, C. A. Farberow, F. Shi, A. C. Alba-Rubio, J. Lu, P. J. Dietrich, X. Gu, C. L. Marshall, P. C. Stair, J. W. Elam, J. T. Miller, F. H. Ribeiro, P. M. Voyles, J. Greeley, M. Mavrikakis, S. L. Scott, T. F. Kuech and J. A. Dumesic, *Angew. Chem., Int. Ed.*, **52**, 13808 (2013).
67. J.-P. Lange, E. van der Heide, J. van Buijtenen and R. Price, *ChemSusChem*, **5**, 150 (2012).
68. R. Mariscal, P. Maireles-Torres, M. Ojeda, I. Sádaba and M. López Granados, *Energy Environ. Sci.*, **9**, 1144 (2016).
69. C. M. Cai, T. Zhang, R. Kumar and C. E. Wyman, *J. Chem. Technol. Biotechnol.*, **89**, 2 (2014).
70. J. Greeley, *Electrochim. Acta*, **55**, 5545 (2010).
71. B. J. O'Neill, J. T. Miller, P. J. Dietrich, F. G. Sollberger, F. H. Ribeiro and J. A. Dumesic, *ChemCatChem*, **6**, 2493 (2014).
72. H. Zhang, Y. Lei, A. J. Kropf, G. Zhang, J. W. Elam, J. T. Miller, F. Sollberger, F. Ribeiro, M. C. Akatay, E. A. Stach, J. A. Dumesic and C. L. Marshall, *J. Catal.*, **317**, 284 (2014).
73. H. Zhang, Y. Lei, A. Jeremy Kropf, G. Zhang, J. W. Elam, J. T. Miller, F. Sollberger, F. Ribeiro, M. Cem Akatay, E. A. Stach, J. A. Dumesic and C. L. Marshall, *J. Catal.*, **323**, 165 (2015).
74. B. J. O'Neill, C. Sener, D. H. K. Jackson, T. F. Kuech and J. A. Dumesic, *ChemSusChem*, **7**, 3247 (2014).
75. J. Lee, D. H. K. Jackson, T. Li, R. E. Winans, J. A. Dumesic, T. F. Kuech and G. W. Huber, *Energy Environ. Sci.*, **7**, 1657 (2014).
76. H. Zhang, C. Canlas, A. Jeremy Kropf, J. W. Elam, J. A. Dumesic and C. L. Marshall, *J. Catal.*, **326**, 172 (2015).
77. D. Liu, D. Zemlyanov, T. Wu, R. J. Lobo-Lapidus, J. A. Dumesic, J. T. Miller and C. L. Marshall, *J. Catal.*, **299**, 336 (2013).
78. Y. J. Pagán-Torres, J. M. R. Gallo, D. Wang, H. N. Pham, J. A. Libera, C. L. Marshall, J. W. Elam, A. K. Datye and J. A. Dumesic, *ACS Catal.*, **1**, 1234 (2011).
79. J. J. Bozell, *Science*, **329**, 522 (2010).
80. J. C. Serrano-Ruiz, D. Wang and J. A. Dumesic, *Green Chem.*, **12**, 574 (2010).
81. J.-P. Lange, R. Price, P. M. Ayoub, J. Louis, L. Petrus, L. Clarke and H. Gosselink, *Angew. Chem., Int. Ed.*, **49**, 4479 (2010).
82. C.-J. Pan, M.-C. Tsai, W.-N. Su, J. Rick, N. G. Akalework, A. K. Agegnehu, S.-Y. Cheng and B.-J. Hwang, *J. Taiwan Inst. Chem. E.*, **74**, 154 (2017).
83. D. E. Resasco and G. L. Haller, *J. Catal.*, **82**, 279 (1983).
84. J. Santos, J. Phillips and J. A. Dumesic, *J. Catal.*, **81**, 147 (1983).
85. S. J. Tauster, *Acc. Chem. Res.*, **20**, 389 (1987).
86. J. A. Dumesic, S. A. Stevenson, R. D. Sherwood and R. T. K. Baker, *J. Catal.*, **99**, 79 (1986).
87. S. Zander, E. L. Kunkes, M. E. Schuster, J. Schumann, G. Weinberg, D. Teschner, N. Jacobsen, R. Schlögl and M. Behrens, *Angew. Chem., Int. Ed.*, **52**, 6536 (2013).
88. R. Naumann d'Alnoncourt, M. Friedrich, E. Kunkes, D. Rosenthal, F. Girgsdies, B. Zhang, L. Shao, M. Schuster, M. Behrens and R. Schlögl, *J. Catal.*, **317**, 220 (2014).
89. A. Bruix, J. A. Rodriguez, P. J. Ramírez, S. D. Senanayake, J. Evans, J. B. Park, D. Stacchiola, P. Liu, J. Hrbek and F. Illas, *J. Am. Chem. Soc.*, **134**, 8968 (2012).
90. G. Melaet, W. T. Ralston, C.-S. Li, S. Alayoglu, K. An, N. Musselwhite, B. Kalkan and G. A. Somorjai, *J. Am. Chem. Soc.*, **136**, 2260 (2014).
91. L. R. Baker, G. Kennedy, M. Van Spronsen, A. Hervier, X. Cai, S. Chen, L.-W. Wang and G. A. Somorjai, *J. Am. Chem. Soc.*, **134**, 14208 (2012).
92. J. Lee, S. P. Burt, C. A. Carrero, A. C. Alba-Rubio, I. Ro, B. J. O'Neill, H. J. Kim, D. H. K. Jackson, T. F. Kuech, I. Hermans, J. A. Dumesic and G. W. Huber, *J. Catal.*, **330**, 19 (2015).
93. N. M. Eagan, J. P. Chada, A. M. Wittrig, J. S. Buchanan, J. A. Dumesic and G. W. Huber, *Joule*, **1**, 178 (2017).
94. H. N. Pham, A. E. Anderson, R. L. Johnson, K. Schmidt-Rohr and A. K. Datye, *Angew. Chem., Int. Ed.*, **51**, 13163 (2012).
95. H. Xiong, H. N. Pham and A. K. Datye, *J. Catal.*, **302**, 93 (2013).
96. H. Xiong, M. Nolan, B. H. Shanks and A. K. Datye, *Appl. Catal. A-Gen.*, **471**, 165 (2014).
97. H. Xiong, T. J. Schwartz, N. I. Andersen, J. A. Dumesic and A. K. Datye, *Angew. Chem., Int. Ed.*, **54**, 7939 (2015).
98. F. Héroguel, L. Silvioli, Y.-P. Du and J. S. Luterbacher, *J. Catal.*, **358**, 50 (2018).
99. J.-P. Lange and V. Otten, *J. Catal.*, **238**, 6 (2006).
100. J.-P. Lange and V. Otten, *Ind. Eng. Chem. Res.*, **46**, 6899 (2007).
101. N. M. Bertero, A. F. Trasarti, C. R. Apesteguía and A. J. Marchi, *Appl. Catal. A-Gen.*, **458**, 28 (2013).
102. Z. Luo, Y. Wang, M. He and C. Zhao, *Green Chem.*, **18**, 433 (2016).
103. T.-S. Nguyen, D. Laurenti, P. Afanasiev, Z. Konuspayeva and L. Piccolo, *J. Catal.*, **344**, 136 (2016).
104. M. B. Griffin, G. A. Ferguson, D. A. Ruddy, M. J. Biddy, G. T. Beckham and J. A. Schaidle, *ACS Catal.*, **6**, 2715 (2016).
105. Q. Tan, G. Wang, A. Long, A. Dinse, C. Buda, J. Shabaker and D. E. Resasco, *J. Catal.*, **347**, 102 (2017).
106. P. A. Zapata, J. Faria, M. P. Ruiz, R. E. Jentoft and D. E. Resasco, *J. Am. Chem. Soc.*, **134**, 8570 (2012).
107. P. A. Zapata, Y. Huang, M. A. Gonzalez-Borja and D. E. Resasco, *J. Catal.*, **308**, 82 (2013).
108. T. van Haasterecht, C. C. I. Ludding, K. P. de Jong and J. H. Bitter,

*J. Catal.*, **319**, 27 (2014).
109. J. H. Vleeming, B. F. M. Kuster, G. B. Marin, F. Oudet and P. Courtine, *J. Catal.*, **166**, 148 (1997).
110. L. Ahonen and O. H. Tuovinen, *Hydrometallurgy*, **37**, 1 (1995).
111. B. Beverskog and I. Puigdomenech, *Corros. Sci.*, **39**, 969 (1997).
112. D. A. Palmer, P. Bénézeth, C. Xiao, D. J. Wesolowski and L. M. Anovitz, *J. Solution Chem.*, **40**, 680 (2011).
113. A. G. Gayubo, B. Valle, A. T. Aguayo, M. Olazar and J. Bilbao, *Energy Fuels*, **23**, 4129 (2009).
114. C. Aellig, D. Scholz, P. Y. Dapsens, C. Mondelli and J. Pérez-Ramírez, *Catal. Sci. Technol.*, **5**, 142 (2015).
115. B. M. Moreno, N. Li, J. Lee, G. W. Huber and M. T. Klein, *RSC Adv.*, **3**, 23769 (2013).
116. L. Vilcocq, A. Cabiac, C. Especel, S. Lacombe and D. Duprez, *J. Catal.*, **320**, 16 (2014).
117. D. M. Alonso, S. G. Wettstein and J. A. Dumesic, *Chem. Soc. Rev.*, **41**, 8075 (2012).

Dr. Jechan Lee received his Ph.D. in chemical engineering from University of Wisconsin-Madison in 2015. He is currently an assistant professor in Department of Environmental and Safety Engineering at Ajou University. His research interests are in the areas of catalysis, biorefinery, $CO_2$ utilization, and waste-to-energy. He is co-authored more than 60 SCI(E) papers.

Dr. Lin received his Ph.D. from the Department of Earth and Environmental Engineering at Columbia University (USA). He is currently working as an Associate Professor in the Department of Environmental Engineering. His research focuses on development of advanced materials and catalysts for energy and environmental applications. In the past few years, he has been becoming one of leading experts for environmental applications of metal organic frameworks (MOFs) and their derivatives. He has also served as editors and editorial members for more than 10 journals and reviewers for more than 80 high-impact journals. Dr. Lin has co-authored more than 105 SCI journal papers.